Available online at www.sciencedirect.com
ScienceDirect
Journal of Power Sources 174 (2007) 970–975
JOURNAL OF POWER SOURCES
www.elsevier.com/locate/jpowsour

Short communication

How dynamic is the SEI?

H. Bryngelsson, M. Stjerndahl, T. Gustafsson, K. Edström *

Department of Materials Chemistry, Ångström Laboratory, Uppsala University, Box 538, SE-751 21 Uppsala, Sweden

Available online 23 June 2007

Abstract

The surface chemistry of graphite and intermetallic AlSb has been studied by XPS (X-ray photoelectron spectroscopy) in a Li-ion battery context using $LiPF_6$ in EC/DEC as electrolyte. The main results for graphite are as follows: the SEI (solid electrolyte interphase) is different for the lithiated state after 3 cycles (0.01 V) compared to the delithiated state (1.5 V); after 50 cycles the SEI is thicker; there are more Li_2CO_3 or semi-carbonates on the surface of the delithiated sample (1.5 V) than on the lithiated sample (0.01 V); LiF is continuously formed during the first cycles but a steady state is reached after 50 cycles; a new peak in the C 1s spectra indicating a fluorine-containing compound is found at high photon energies (292 eV). The main results for AlSb are as follows: the SEI is different for the lithiated state (0.01 V) compared to the delithiated state (1.2 V) after 3 cycles; after 50 cycles the surface layer thickness is slightly larger but significantly thinner than for graphite; contrary to graphite, more Li_2CO_3 or semi-carbonates are found on the surface of the lithiated sample; also here a new peak indicating a fluorine-containing compound is found in the C 1s spectra at 292 eV. The general result is that the SEI has many similar features between graphite and AlSb but also important differences. The carbonaceous layer is dynamically shifting in chemical composition during cycling for both samples.

Keywords: Li-ion battery; Intermetallic anode; SEI; Graphite; XPS; AlSb

1. Introduction

Numerous studies have been carried out on the characterisation of the SEI (solid electrolyte interphase) on the negative electrode in Li-ion batteries [1–18]. This interface is protecting graphite from exfoliation and co-intercalation of solvent molecules at the same time as it is consuming lithium-ions in its formation at potentials below 0.8 V versus Li^0/Li^+. The composition and morphology has been long debated and there are several different models proposed [5,6,9]. It is clear that the layer consists of both inorganic and organic species and that there is a dense layer close to the particle surface with a thickness of about 20 Å and on top of this a porous organic layer ranging up to ~800 Å in thickness [12]. In this matrix inorganic crystalline substances such as, for example, LiF are embedded. The chemical composition at a detailed level is dependent on the type of salt present in the electrolyte, temperature, type and surface chemistry of the graphite, to mention some parameters [9,11–19].

SEI phenomena have not been studied for intermetallic anodes in the same detail as for graphite. The reported studies show, however, that the SEI is different to that of graphitic compounds both in terms of chemical composition and morphology [20,21]. In general, the amount of LiF is lower than for graphite. The surface structure of graphite seems to have a catalytic effect on the formation of LiF which is not observed in the same large amounts in SEI for intermetallics cycled in Li-ion batteries using the same type of electrolytes.

In spite of all this available information, there are still issues regarding the electrode/electrolyte interface formation in Li-ion batteries that have to be addressed. Why are some types of SEI layers more effective than others? Why can low irreversible loss of lithium during cycling still lead to long-term cycling stability of the electrode? How dynamic is the SEI during cycling? In this paper we are studying how the SEI will develop during cycling for both graphite and an intermetallic system (AlSb). We are basing our observations on the use of XPS (X-ray photoelectron spectroscopy) as the characterisation technique. Despite the experimental drawbacks of XPS (risk of radiation damage, the need of high vacuum conditions, etc.), this is the technique to use to get information of layers that are as thin as the SEI (below 50 Å).

* Corresponding author.
E-mail address: Kristina.Edstrom@mkem.uu.se (K. Edström).

0378-7753/$ – see front matter © 2007 Elsevier B.V. All rights reserved.
doi:10.1016/j.jpowsour.2007.06.050

2. Experimental

2.1. Graphite

The graphite used is a synthetic graphite, Lx 311P, from Toyo Tanso. The particle size is around 20 μm with a flake-like particle morphology.

2.2. Preparation of AlSb

A high-frequency furnace was used for the drop synthesis of AlSb. An ingot made from aluminium was heated to its melting point (660 °C) under argon and at a pressure of 300 mbar. Bits of antimony were dropped into the melt until the proportion 1:1 with aluminium was reached. The AlSb ingot was cooled and ground by hand before ball milling. The powder was mixed with 3 wt% graphite as a solid lubricant in a glove box with an argon atmosphere (<3 ppm H_2O and O_2) and placed in a SPEX (CertiPrep) stainless steel vessel; the vessel was sealed with an o-ring to maintain the inert atmosphere. High-energy ball milling was performed for 16 h at room temperature. XRD patterns of the AlSb sample were collected on a Siemens D5000 diffractometer using Cu Kα radiation before and after ball milling.

2.3. Preparation of electrodes and Li-ion batteries

Graphite electrodes were prepared by mixing 80 wt% Lx 311P (Toyo Tanso), 10% acetylene black (Chevron) carbon powder and 10 wt% binder (polyvinylidene difluoride, PVDF) dissolved in *N*-methyl pyrrolidone (NMP). AlSb electrodes were manufactured by preparing a mixture of 80 wt% ball milled AlSb powder, 10 wt% acetylene black carbon powder and 10 wt% PVDF binder in NMP. The resulting slurry was coated on a copper foil and cut into 3.14 cm^2 circular discs. The electrodes were dried at 120 °C in vacuum prior to use. The typical loading of active material was in the range of 6–7 mg cm^{-2}. Electrochemical (coffee-bag type) cells were assembled in the glove box by laminating the graphite or AlSb electrodes with a glass–wool separator soaked in electrolyte, which consisted of 1 M $LiPF_6$ dissolved in ethylene carbonate (EC, Merck battery grade) and diethyl carbonate (DEC, Merck battery grade) in a volumetric ratio of 2 to 1. The $LiPF_6$ salt was vacuum dried at 80 °C in the glove box prior to use; the solvents were used as-received. Lithium-foil was used as the counter electrode. The laminate was vacuum sealed in a polymer coated aluminium foil with attached nickel contacts.

The cells were galvanostatically cycled, with a Digatron BTS-600 Battery Tester, at room temperature, with a current density corresponding to a charge or discharge time of 10 h. Because of the high irreversible capacity in the first cycle for AlSb the first discharge was set to 27 h, yielding a discharge time of 10 h in the following cycles. For AlSb the charge cut-off potential was 1.20 V and the discharge cut-off potential was either 0.50 V or 0.01 V. For graphite the charge cut-off potential was 1.50 V and the discharge cut-off potential was 0.01 V.

2.4. XPS characterisation

Prior to surface analysis, all electrodes were removed from the battery and immersed in DEC for 30 min within the glove box. The DEC rinse was used to remove electrolyte salt residues that are not inherent to the SEI. The electrodes were then dried at room temperature for 1 h under reduced pressure. The electrodes were mounted on a sample holder in the glove box and transported to the analysis chamber using a specially designed transport vessel to avoid contamination from air. Measurements were performed on a PHI 5500 system, using monochromatized Al Kα, at 1486.6 eV, and at a base pressure of 5×10^{-10} Torr and a working pressure $<5 \times 10^{-9}$ Torr. High-resolution spectra of the C 1s and F 1s regions were obtained with a pass-energy of 23.5 eV.

The binding energy scales for the high-resolution C 1s spectra were calibrated with the carbon black peak set to 284.4 eV. When the carbon black peak was not observed, the sample spectra were calibrated with the main C 1s peak set to 286.7 eV which was the binding energy determined for the main C 1s peak in spectra containing graphite. For all spectra the intensities were normalised versus the main C 1s peak to allow comparison (from the relative peak intensities) between the same elements in different electrodes. Peak assignments were made based on detailed curve fitting of the recorded spectra using Gaussian–Lorenzian peak shapes and a Shirley function background correction, together with reference measurements.

The binding energies for the high-resolution F 1s spectra were calibrated with the LiF peak set to 686.6. Here the spectra were normalised versus the LiF peak.

3. Results

3.1. Graphite

The synthetic graphite showed an irreversible capacity loss of 12.5% during the first cycle (see Fig. 1). The different staging phases during lithiation/delithiation are clearly observed and the

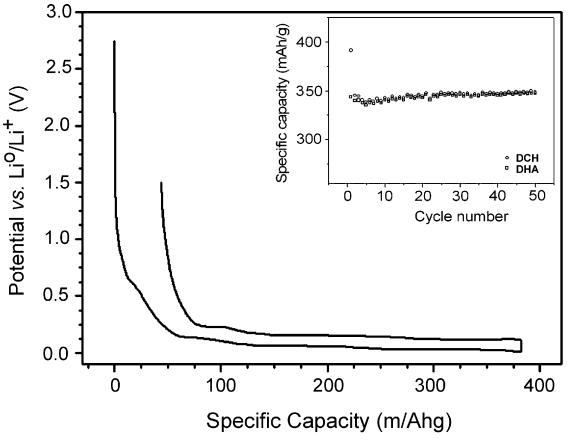

Fig. 1. The first cycle of galvanostatically (*C*/10) cycled graphite. The irreversible capacity loss is 12.5% in the first cycle. The first 50 cycles are shown in the inset.

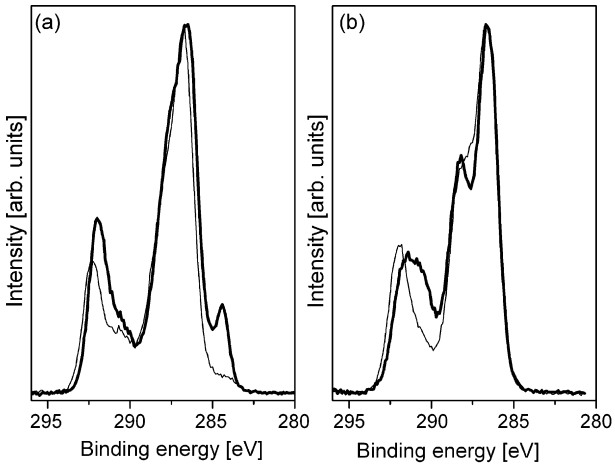

Fig. 2. The C 1s spectra of graphite: lithiated (thin line) and delithiated (thick line) after 3 cycles (a) and after 50 cycles (b).

cycling stability is high with a capacity of ∼350 mAh g^{-1} for at least 50 cycles at a cycling rate of *C*/10.

3.2. C 1s XPS spectra of graphite cycled three times

In Fig. 2a the C 1s XPS spectra of a graphite electrode in its lithiated and delithiated state after 3 cycles is shown. The spectrum reveals the functional groups typical for the SEI on graphite (Table 1). The main observed difference between the lithiated and the delithiated state is the thickness of the layer as determined by the observation of the carbon black at 284.4 eV. For both samples the SEI is thinner than the penetration depth of the XPS analysis (∼50 Å), but the SEI is significally thinner for the delithiated sample according to the intensity of the carbon black peak (relative to the main C 1s peak). This difference can be a true dynamic behaviour with a thickening of the SEI layer at lower potentials and a thinning-out of the layer at 1.5 V as in the delithiated state.

The functional groups present in the SEI are the same for the lithiated and delithiated samples, but the ratio between the groups differ. Extra attention can be paid to the peak at 292 eV. This peak is not present for graphites that have been cycled in EC/DMC. One explanation for this observation can be that there are reactions occurring between electrolyte and the binder. There are only few C–F compounds reported that have binding energies at these high eV (i.e. R–CF_2R [11] and –($CH_2CH(OC(O)CF_3)$)$_n$– [22]). The exact nature of the species found here remains to be understood.

3.3. C 1s XPS spectra of graphite cycled 50 times

The C 1s spectra of lithiated and delithiated graphite that have cycled 50 times at *C*/10 are shown in Fig. 2b. Here, the SEI layers are in both cases thicker than that formed after 3 cycles (as determined by the lack of visibility of the carbon black peak at 284.4 eV). It has been shown earlier that the largest irreversible growth of the SEI occurs during the first cycle, but that at least 5 cycles, if not more, are needed for a complete growth of the layer. The subtle differences observed for the graphite electrodes cycled three times (Fig. 2a) are now more pronounced. The peak at 291 eV, is more pronounced for the delithiated than the lithiated sample. This peak can be attributed to either Li_2CO_3 or to semi-carbonates. The surface species of new fluorine-containing compounds identified at 292 eV also exist after 50 cycles. The amount has not increased, however, compared to the growth of some of the other C 1s species.

3.4. F 1s on graphite

In the F 1s spectra of graphite cycled 3 and 50 times, Fig. 3a and b, two main peaks can be identified. At 686.5 eV the peak of

Table 1
Summary of XPS peak assignments

Assignments	Measured binding energy (eV)				
	C 1s	O 1s	F 1s	Sb $3d_{3/2}$	Sb $3d_{5/2}$
Carbon black	284.4 [27]				
Hydrocarbon	285.0 [11]				
–(CH_2CH_2O)$_n$–	286.5 [11]	533 [11]			
Li_2CO_3	290 [11]	532[a]			
R–CH_2OCO_2Li	288 [24]	533.5 [24]			
R–CH_2OCO_2Li	290–291 [24]	532[a]			
R–CH_2OLi	288 [25]	532[a]			
–(CH_2–CF_2)$_n$–	286.2 [28]		687.8[i]		
–(CH_2–CF_2)$_n$–	290.7 [28]		687.8[i]		
R–CF_2–R	290.7–292 [11,28]		688.2 [22]		
–(CH_2CH–($OC(O)CF_3$))$_n$–	292.7 [22]		688.2 [22]		
AlSb				537.7 [26]	528.6 [26]
Li_3Sb					526.9
LiF			686.5 [9]		
$LiPF_6$			688 [11]		
Li_xPF_y			687–688 [11]		
$Li_xPF_yO_z$		∼535 [11]			

[a] With careful consideration of experimental data and Refs. [11,24,25,29] we have assigned the peak to 532 eV.

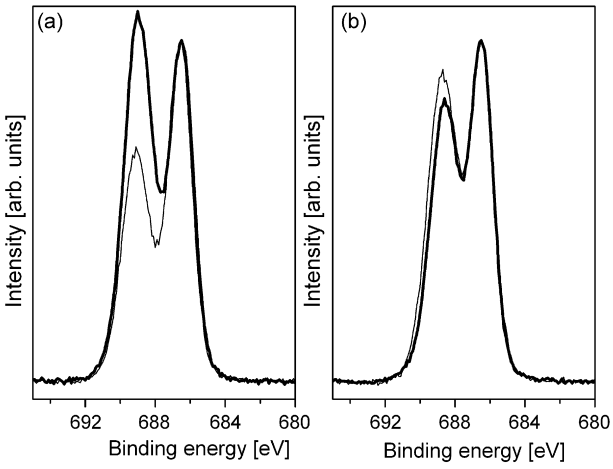

Fig. 3. The F 1s spectra of graphite: lithiated (thin line) and delithiated (thick line) after 3 cycles (a) and after 50 cycles (b).

LiF is identified and at 689 eV both salt and salt residues, $LiPF_6$ or $Li_xP_yF_z$, is coinciding with the signal of fluorine in PVdF, see Table 1. The normalisation of the peaks to LiF allows a comparison between the different samples. Comparing the 686.5 eV peak with the peak at 689 eV for the electrode cycled three times (Fig. 3a), the amount of LiF on the surface is larger for the lithiated sample than that on the delithiated sample.

The observed increase of LiF for the electrode in its lithiated state (compared to the 689 eV peak) could also be a result of an increasing SEI formation at lithiation as is also seen in the C 1s spectrum where the carbon black decreases. The peak at 689 eV (PVdF) is decreasing because of an increased amount of carbonaceous species at the surface, indicating that the SEI is still growing.

After 50 cycles, the relative intensities of the peaks are the same for the lithiated and the delithiated sample, indicating a steady state of fluorine species in the SEI.

3.5. AlSb

The first cycle of AlSb cycled between 1.2 V and 0.5 V and that of AlSb cycled between 1.2 V and 0.01 V, are shown in Fig. 4. During lithium alloying of AlSb, aluminium is directly extruded and lithium is alloying with antimony according to Eq. (1). No intermediate $Li_xAl_{1-x}Sb$ phase is formed [23]:

$$3Li + Sb \Leftrightarrow Li_3Sb \quad (1)$$

The cycling between 1.2 V and 0.5 V is stable for more than 50 cycles while that between 1.2 V and 0.01 V show a continuous capacity fade (both are based on cycling rates of *C*/10). After 50 cycles the cycling capacity has dropped with 33% from the 2nd to the 50th cycle for the sample cycled to 0.5 V and with 47% for the sample cycled to 0.01 V.

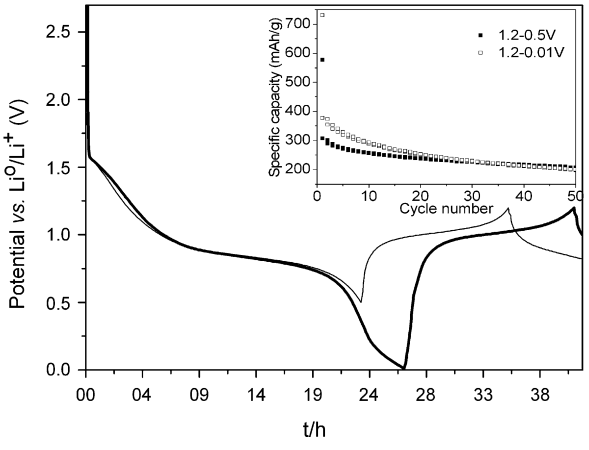

Fig. 4. The first cycle of AlSb cycled with a voltage window of 1.2–0.5 V and 1.2–0.01 V. The first 50 cycles are shown in the inset.

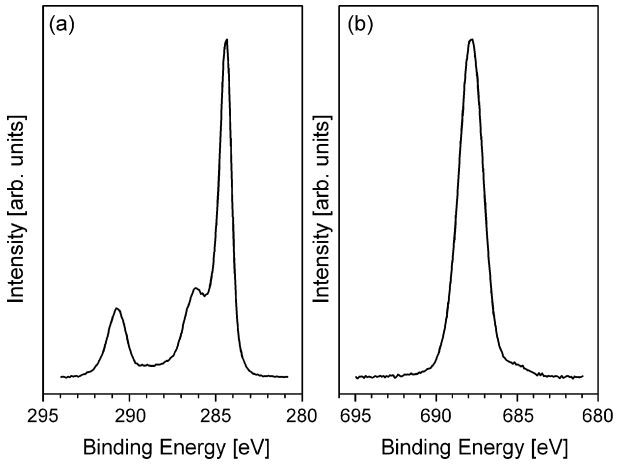

Fig. 5. The C 1s spectrum (a) and the F 1s spectrum (b) of an AlSb electrode consisting of 80% active material. Ten percent of carbon black and 10% PVDF binder.

The C 1s and F 1s spectra for an uncycled AlSb electrode are shown in Fig. 5. In the C 1s spectra the carbon black peak is shown at 284.4 eV. The PVDF is shown at 291 eV in the C 1s spectra and at 687.8 eV in the F 1s spectra.

3.6. C 1s spectra of delithiated AlSb after 3 cycles

The C 1s spectra of delithiated AlSb electrodes after 3 cycles using two different voltage windows are shown in Fig. 6a and b.

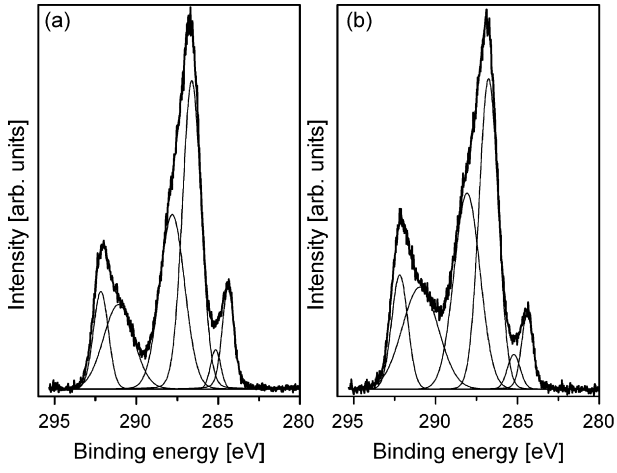

Fig. 6. The C 1s spectrum of an AlSb electrode in its delithiated state after 3 cycles with a voltage window of 1.2–0.5 V (a) and 1.2–0.01 V (b), respectively.

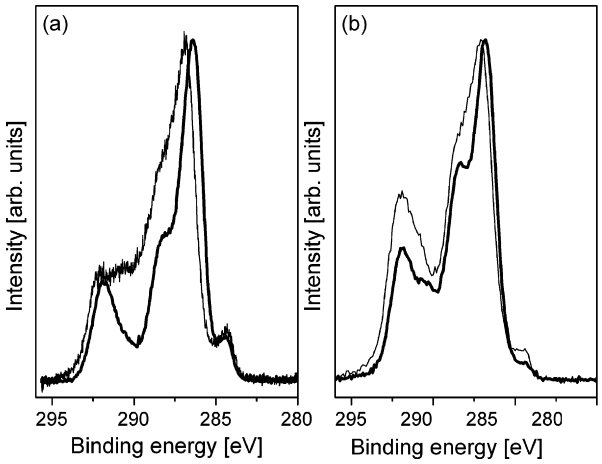

Fig. 7. The C 1s spectrum of an AlSb electrode in its lithiated (thin line) and delithiated state (thick line) after 50 cycles with a voltage window of 1.2–0.5 V (a) and 1.2–0.01 V (b).

The surface species components after 3 cycles are very similar to those of the graphite surface (Fig. 2a). The ratio between the different functional groups is, however, different. The surface of AlSb contains less –C–O– species than the graphite electrodes. This holds for both the electrode cycled between 1.2 V and 0.5 V (Fig. 6a) and for the electrode cycled between 1.2 V and 0.01 V (Fig. 6b). Smaller amounts of alkyl carbonates are thus formed on the intermetallic compound.

The new fluorine-containing groups present at 292 eV show that the surface reaction between binder and electrolyte is independent of electrode material and its surface structure.

3.7. C 1s spectra of lithiated and delithiated AlSb after 50 cycles

Comparing first the lithiated/delithiated surface chemistries of the sample cycled 50 times between 1.5 V and 0.5 V a difference is observed at 290–291. The surface of the lithiated electrodes contain more Li_2CO_3 (and/or R–CH_2OCO_2Li and or (–(CH_2–CF_2)$_n$–) species (Fig. 7a and b and Table 1). This is

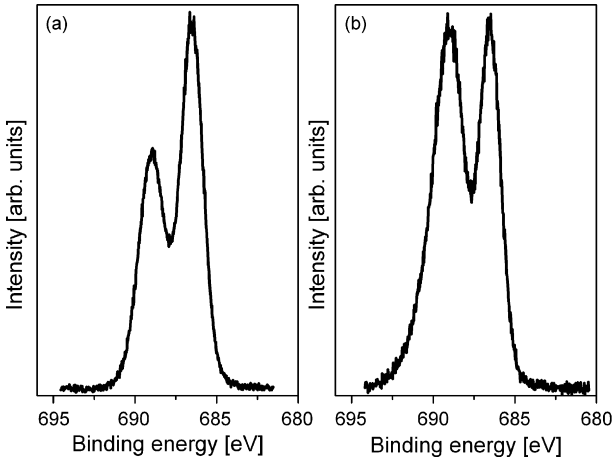

Fig. 8. The F 1s spectrum of an AlSb electrode in its delithiated state after 3 cycles with a voltage window of 1.2–0.5 V (a) and 1.2–0.01 V (b), respectively.

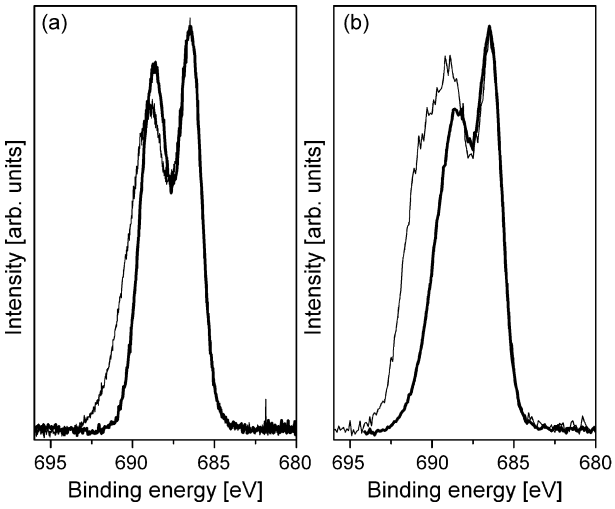

Fig. 9. The F 1s spectrum of an AlSb electrode in its lithiated (thin line) and delithiated state (thick line) after 50 cycles with a voltage window of 1.2–0.5 V (a) and 1.2–0.01 V (b).

also seen for the sample cycled between 1.5 V and 0.01 V, but with the largest difference for the electrode cycled between 1.5 V and 0.5 V. The thickness of the SEI is not changing significantly after 50 cycles but the SEI is still dynamic.

Unlike graphite (Fig. 2b), the carbon black peak is still visible, irrespective of cycling range, after 50 cycles (Fig. 7a and b) proving a thinner SEI than for graphite.

The new fluorine-containing groups at 292 eV are still present after 50 cycles.

3.8. F 1s spectra of AlSb

In Fig. 8 the F 1s spectra for an AlSb electrode in its delithiated state after 3 cycles are shown. When the electrodes have been galvanostatically cycled for 3 cycles, the amount of LiF seem to be larger for the electrode cycled between 1.2 V and 0.5 V (Fig. 8a) than for the electrode cycled between 1.2 V and 0.01 V (Fig. 8b).

Another explanation is that additional fluorinated species, with higher binding energies, are formed on the surface at low potential upon cycling. This is supporting the observation in the C 1s spectrum of a new carbon–fluorine compound at high photon energy (292 eV). The width of the peak at higher binding energies is broadened with cycling. The broadening of the peak at higher energies is getting more pronounced after 50 cycles (Fig. 9), especially when the electrode is cycled between 1.2 V and 0.01 V (Fig. 9b).

4. Conclusions

The surface characterisation of both graphite and AlSb show the SEI to be dynamic in that sense that some carbonaceous compounds are present in the lithiated state and some in the delithiated state. Even though XPS will not give more than a post-mortem picture of the SEI of the two compared anode materials for Li-ion batteries, we have shown some important trends.

- We have established that the thickness of the carbonaceous layer is larger for graphite than for AlSb upon long time cycling (here 50 cycles).
- After 3 cycles, the thickness of the SEI is larger for the lithiated than the delithiated graphite.
- For AlSb the layer is thinner than the penetration depth of the XPS beam (50 Å) also after 50 cycles.
- At 287.5 eV, the alkyl carbonates are changing with cycling and with type of anode material used. The results show a growth of these compounds at the lithiated state for AlSb after 50 cycles compared to the delithiated state.
- We have also established that after 50 cycles Li_2CO_3 or R–COCO_2–R compounds at 291 eV are more important for the delithiated than for the lithiated graphite. After 3 cycles the pattern is less clear. The opposite behaviour is observed for AlSb.
- We have seen that LiF is not dynamically changing with cycling but rather that the amount of salt is increasing as a function of cycling.
- We have observed a new carbon–fluorine-containing compound to be present at 292 eV in C 1s in all electrodes cycled in EC/DEC.

The results of this study show that during cycling chemical processes occurs that are dynamic in their characters.

Acknowledgements

This work has been supported by the Swedish Research Council (VR), the Göran Gustafsson Foundation and the Carl Trygger Foundation. Hanna Bryngelsson is also grateful for the support from Ångpanneföreningen. The authors would also like to acknowledge Prof. Josh Thomas for many fruitful discussions and for his interest in this work.

References

[1] E. Peled, J. Electrochem. Soc. 126 (1979) 2047.
[2] E. Peled, D. Golodnitsky, G. Ardel, J. Electrochem. Soc. 144 (1997) L208.
[3] E. Peled, D. Golodnitsky, C. Menachem, D. Bar-Tow, J. Electrochem. Soc. 145 (1998) 3482.
[4] D. Aurbach, B. Markovsky, I. Weissman, E. Levi, Y. Ein-Eli, Electrochim. Acta 45 (1999) 67.
[5] E. Peled, in: J.O. Besenhard (Ed.), Handbook of Battery Materials, Wiley-VCH, Weinheim, 1999.
[6] D. Aurbach, Nonaqueous Electrochemistry, Marcel Dekker, New York, 1999.
[7] R. Yazami, Electrochim. Acta 45 (1999) 87.
[8] D. Bar-Tow, E. Peled, L. Burstein, J. Electrochem. Soc. 146 (1999) 824.
[9] A.M. Andersson, K. Edström, J. Electrochem. Soc. 148 (2001) A1100.
[10] E. Peled, D. Bar Tow, A. Merson, A. Gladkichm, L. Burstein, D. Golodnitsky, J. Power Sources 97/98 (2001) 52.
[11] A.M. Andersson, M. Herstedt, A. Bishop, K. Edstrom, Electrochim. Acta 47 (2002) 1885.
[12] A.M. Andersson, A. Henningsson, H. Siegbahn, U. Jansson, K. Edstrom, J. Power Sources 119–121 (2003) 522.
[13] M. Herstedt, A.M. Andersson, H. Rensmo, H. Siegbahn, K. Edstrom, Electrochim. Acta 49 (2004) 4939.
[14] M. Herstedt, D.P. Abraham, J.B. Kerr, K. Edstrom, Electrochim. Acta 49 (2004) 5097.
[15] A. Augustsson, M. Herstedt, J.-H. Guo, K. Edstrom, G.V. Zhuang, P.N. Ross Jr., J.-E. Rubensson, J. Nordgren, Phys. Chem. Chem. Phys. 6 (2004) 4185.
[16] M. Herstedt, H. Rensmo, H. Siegbahn, K. Edstrom, Electrochim. Acta 49 (2004) 2351.
[17] S. Leroy, F. Blanchard, R. Dedryvere, H. Martinez, B. Carre, D. Lemordant, D. Gonbeau, Surf. Interf. Anal. 37 (2005) 773.
[18] K. Edstrom, M. Herstedt, D.P. Abraham, J. Power Sources 153 (2006) 380.
[19] M.E. Spahr, H. Buqa, A. Wuersig, D. Goers, L. Hardwick, P. Novak, F. Krumeich, J. Dentzer, C. Vix-Guterl, J. Power Sources 153 (2006) 300.
[20] M.R. Wagner, P.R. Raimann, A. Trifonova, K.-C. Moeller, J.-O. Besenhard, M. Winter, Electrochem. Solid-State Lett. 7 (2004) A201.
[21] D.-T. Shieh, J. Yin, K. Yamamoto, M. Wada, S. Tanase, T. Sakai, J. Electrochem. Soc. 153 (2006) A106.
[22] G. Beamson, D. Briggs, High Resolution XPS of Organic Polymers: The Scienta ESCA300 Database, Wiley Interscience, 1992.
[23] M. Stjerndahl, H. Bryngelsson, T. Gustafsson, J.T. Vaughey, M.M. Thackeray, K. Edström, Electrochim. Acta 52 (2007) 4947.
[24] G. Zhuang, Y. Chen, P.N. Ross, Langmuir 15 (1999) 1470.
[25] L.J.J. Rendek, G.S. Chottiner, D.A. Scherson, J. Electrochem. Soc. 149 (2002) E408.
[26] W.E. Morgan, W.J. Stec, J.R. Van Wazer, Inorg. Chem. 12 (1973) 953.
[27] M. Herstedt, M. Stjerndahl, A. Nytén, T. Gustafsson, H. Rensmo, H. Siegbahn, N. Ravet, M. Armand, J.O. Thomas, K. Edström, Electrochem. Solid-State Lett. 6 (2003) A202.
[28] A. Tressaud, E. Papirer, T. Moguet, G. Nanse, P. Fioux, Carbon 35 (1997) 175.
[29] R. Dedryvére, L. Gireud, S. Grugeon, S. Laruelle, J.-M. Tarascon, D. Gonbeau, Phys. Chem. 109 (2005) 15868.